PARAMETRIC STUDY ON SUBOPTIMAL CONTROL FOR DRAG REDUCTION IN TURBULENT CHANNEL FLOW

Jung-Il Choi
Department of Mechanical Engineering, KAIST
373-1, Kusong-dong, Yusong-gu, Taejon, 305-701, Korea
jichoi@kaist.ac.kr

Hyung Jin Sung*
Department of Mechanical Engineering, KAIST
373-1, Kusong-dong, Yusong-gu, Taejon, 305-701, Korea
hjsung@kaist.ac.kr

ABSTRACT

A systematic analysis is made of suboptimal control for drag reduction. The influence of the amplitude of actuation (A) and the time scale of actuation (Δt_a^+) is evaluated. Two wall sensing variables are employed ($\partial w/\partial y|_w$ and $\partial p/\partial z|_w$), with two actuations (ϕ_2 and ϕ_3). It is found that the effect of A and Δt_a^+ on the drag reduction rate (D_r) is significant. The near-wall behaviors of flow structure are analyzed to characterize the drag reduction. An optimal time scale is obtained at $\Delta t_a^+ \simeq 1$.

INTRODUCTION

The role of near-wall streamwise vortices has been found to be very important in a wall-bounded turbulent flow. The downward sweep motion induced by streamwise vortices very near wall is closely correlated with skin friction (Kim et al., 1987). In order to achieve a reduction of skin friction, the management of near-wall streamwise vortices has been a target of control strategies. In Lee, Kim and Choi (1998), hereafter referred to as LKC, a feedback control law was proposed for drag reduction by applying a suboptimal control theory to turbulent channel flows. The main aim of their study was to derive a feedback control law by using the sensing quantities only at the wall, not inside the flow. Other recent studies on the active control have required velocity information inside the flow, which may be impractical for real implementations (Choi et al., 1994 and Bewley et al., 1993).

*This work was supported by a grant from the National Research Laboratory of the Ministry of Science and Technology, Korea. The authors gratefully acknowledge valuable discussions with Prof. Changhoon Lee.

In the suboptimal procedure of LKC, two suboptimal control laws were devised which require the local distributions of the spanwise velocity gradient ($\partial w/\partial y|_w$) or the spanwise wall pressure gradient ($\partial p/\partial z|_w$). These control laws give us to know only the phase information of the control input at a local time. This is because 'suboptimal' implies only 'spatial optimal' in a control region. Since LKC's study was confined to a spatial optimum in a control surface, an actuation time scale (Δt_a^+) was not considered. Furthermore, the amplitude of the control input (A) was assumed to be a proper constant in the course of analytic formulation.

In the present study, the influence of the amplitude of actuation (A) and the time scale of actuation (Δt_a^+) is evaluated by applying a suboptimal control procedure. Two sensing parameters are chosen, $\partial w/\partial y|_w$ and $\partial p/\partial z|_w$, in connection with two actuations, i.e. , the wall normal blowing and suction (ϕ_2) and the sliding wall velocity (ϕ_3), respectively. Main emphasis is placed on the identification of the responses of near-wall layer dynamics to the control parameters. The active cancellation in opposition to the near-wall velocity at a detection layer is also employed to evaluate the effectiveness of the suboptimal control scheme.

SUBOPTIMAL CONTROL PROCEDURE

For an incompressible turbulent flow, the Navier-Stokes equations and continuity equation can be written as

$$\frac{\partial u_i}{\partial t} + \frac{\partial (u_i u_j)}{\partial x_j} = -\frac{\partial p}{\partial x_i} + \frac{1}{Re}\frac{\partial^2 u_i}{\partial {x_j}^2} \quad (1)$$

$$\frac{\partial u_i}{\partial x_i} = 0 \text{ with } u_i|_w = \phi_i(x,z,t) \qquad (2)$$

The actuations (ϕ_i) at the wall are considered, where ϕ_1, ϕ_2 and ϕ_3 are the streamwise sliding, the wall suction/blowing and the spanwise sliding velocity, respectively.

The differential states of the velocity and pressure (θ_i, ρ) are defined using a Fréchet differential,

$$\theta_i = \frac{\mathcal{D}u_i(\phi_i)}{\mathcal{D}\phi_i}\tilde{\phi}_i, \quad \rho = \frac{\mathcal{D}p(\phi_i)}{\mathcal{D}\phi_i}\tilde{\phi}_i \qquad (3)$$

When the spanwise wall shear stress ($\partial w/\partial y|_w$) is chosen as a sensing variable, the following cost functional should be minimized as,

$$\mathcal{J} = \frac{1}{2A\Delta t}\int_S\int_T \left(l\phi_i^2 - \left.\frac{\partial w}{\partial y}\right|_w^2 \right) dtdS \qquad (4)$$

where the integrations are taken over the wall (S) in space over a short duration in time (Δt). l is the relative price of the control. The Fourier representation of the Fréchet differential of the cost functional is

$$\frac{\widehat{\mathcal{D}\mathcal{J}}}{\mathcal{D}\phi}\hat{\tilde{\phi}}_i^* = l\,\hat{\phi}\,\hat{\tilde{\phi}}^* - \left.\widehat{\frac{\partial w}{\partial y}}\right|_w \left.\widehat{\frac{\partial \theta_3}{\partial y}}\right|_w^* \qquad (5)$$

where ($\hat{}$) denotes the Fourier coefficient and the superscript (*) denotes the complex conjugate. To minimize the Fréchet differential of cost functional for an arbitrary $\hat{\tilde{\phi}}_i^*$, i.e. $\frac{\widehat{\mathcal{D}\mathcal{J}}}{\mathcal{D}\phi_i} = 0$, the optimal actuations ($\hat{\phi}_i$) become

$$\hat{\phi}_1 = -C_1\frac{k_1k_3}{k}\left.\widehat{\frac{\partial w}{\partial y}}\right|_w \simeq 0 \qquad (6)$$

$$\hat{\phi}_2 = C_2\frac{i\lambda k_3}{k}\left.\widehat{\frac{\partial w}{\partial y}}\right|_w \simeq C_2'\frac{ik_3}{k}\left.\widehat{\frac{\partial w}{\partial y}}\right|_w \qquad (7)$$

$$\hat{\phi}_3 = -C_3\left(\lambda + \frac{k_3^2}{k}\right)\left.\widehat{\frac{\partial w}{\partial y}}\right|_w \simeq -C_3'\left.\widehat{\frac{\partial w}{\partial y}}\right|_w \qquad (8)$$

where some constants C_i, C_i' are positive scale factors which are restricted within the total power of actuation. Under the assumptions of $k_{max} \sim Re^{3/4}$, where k_{max} corresponds to the Kolmogorov length scale and $u\Delta t/\Delta x \sim O(1)$, it becomes $(2Re/\Delta t)/k^2 \gg 1$. The optimal solutions can be simplified in the right hand side of Eqs. (6)-(8).

Similarly, when the pressure gradient in the spanwise direction is chosen, the cost functional to be minimized is then,

$$\mathcal{J} = \frac{1}{2A\Delta t}\int_S\int_T \left(l\phi_i^2 - \left.\frac{\partial p}{\partial z}\right|_w^2 \right) dtdS. \qquad (9)$$

From the requirement that the Fréchet differential of cost functional be minimized, i.e. $\frac{\widehat{\mathcal{D}\mathcal{J}}}{\mathcal{D}\phi_i} = 0$, the optimal actuations ($\hat{\phi}_i$) become

$$\hat{\phi}_1 = -C_1 i\frac{k_1k_3^2}{k}\hat{p}_w \simeq 0 \qquad (10)$$

$$\hat{\phi}_2 = +C_2\frac{\lambda k_3^2}{k}\hat{p}_w = C_2'\frac{k_3^2}{k}\hat{p}_w \qquad (11)$$

$$\hat{\phi}_3 = -C_3 i\frac{k_3^3}{k}\hat{p}_w \simeq 0 \qquad (12)$$

The actuation in Eq. (12) does not give any contribution to drag reduction. However, a similarity exists between $\partial p/\partial z|_w$ and the streamwise vorticity ($\omega_x|_w$) at the wall (Kim, 1989). The suboptimal control in ϕ_3 with $\partial p/\partial z$ can be modified as

$$\hat{\phi}_3 = -C_3'\left.\widehat{\frac{\partial w}{\partial y}}\right|_w \simeq C_3'\left.\widehat{\frac{\partial p}{\partial z}}\right|_w = iC_3'k_3\hat{p}_w \qquad (13)$$

In the suboptimal procedure of LKC, only the phase information at a local time was provided by a weight distribution between actuators and sensors, e.g., ϕ_2 and $\partial w/\partial y|_w$. Since their study was confined to a spatial optimum in a control surface, an actuation time scale (Δt_a^+) was not taken into consideration. In addition, the amplitude of actuation (A) was assumed to be constant in their analytic formulation. A is defined as the root-mean-square of ϕ_i in a control surface. The sensing and actuation are updated at every Δt_a^+ in the present study.

RESULTS AND DISCUSSION

Direct numerical simulations of turbulent channel flow at low Reynolds number ($Re_\tau = 100$) are performed to apply the suboptimal control scheme. The spectral numerical scheme used in this study is nearly the same as that used in Kim et al.(1987). The domain extends $4\pi\delta \times 2\delta \times 4\pi\delta/3$ in the streamwise, wall-normal, and spanwise directions, in concert with a grid size of $32 \times 65 \times 32$. All the simulations are performed using constant mass flux. Periodic boundary conditions are imposed in the streamwise and spanwise directions. The control is applied to only the bottom wall of the channel.

Before applying the suboptimal control, the active cancellation procedure of Choi et al.(1994) is revisited and applied, which employs blowing and suction in opposition to the wall-normal velocity (ϕ_2) at a detection layer

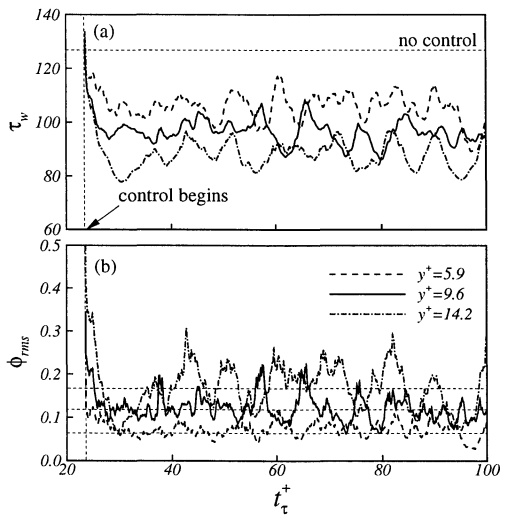

Fig. 1. Time history of (a) streamwise mean shear stress and (b) root-mean-squared values of actuation for ϕ_2.

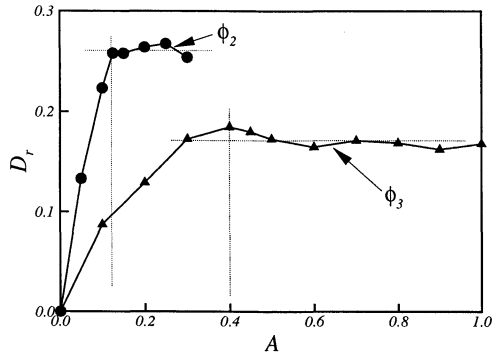

Fig. 2: Effect of A on D_r for $\partial w/\partial y|_w$.

located a small distance from the wall. This is to evaluate the amplitude of actuation in the present suboptimal control. In the active cancellation (Choi et al., 1994 and Hammond et al., 1998), the location of the detection layer is important to achieve an effective drag reduction. In the present study, three detection layers ($y_d^+ = 5.9$, 9.6 and 14.2) are chosen and behaviors of the controlled flows are shown in Fig. 1. As control begins, the controlled mean streamwise shear stress (τ_w) is abruptly reduced and it converges to an asymptotic steady state. The corresponding amplitude of actuation ϕ_{rms} also converges to a quasi-steady state. The maximum drag reduction (τ_w) is obtained at $y_d^+ \simeq 14.2$ among them. As seen in Fig. 1(b), the levels of ϕ_{rms} depend on the detection layers. For example, when the detection layer is selected at $y_d^+ = 9.6$, the asymptotic level of ϕ_{rms} is close to $\phi_{rms} \simeq 0.121$.

Now, the main suboptimal control is performed by the actuation of wall suction and

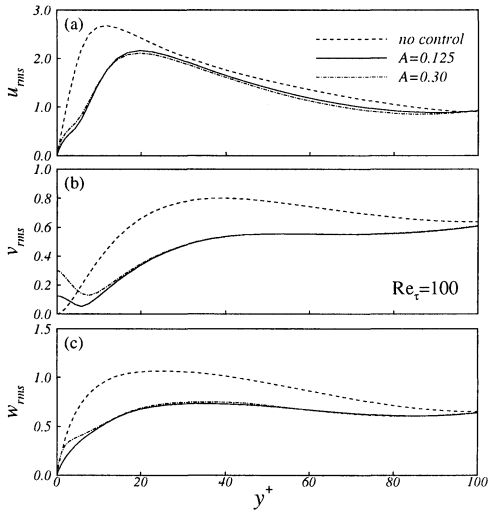

Fig. 3. Root-mean-squared velocity distributions for ϕ_2 and $\partial w/\partial y|_w$. (a) u_{rms} (b) v_{rms} (c) w_{rms}.

blowing (ϕ_2). The spanwise velocity gradient at the wall ($\partial w/\partial y|_w$) is chosen as a sensing variable. The maximization of the spanwise wall shear stress brings on the shrinkage of the near-wall layer dynamics, which is similar to the control of streamwise vorticity near the wall. The drag reduction rate (D_r) is defined as $D_r = (\tau_{no} - \tau_c)/\tau_{no}$, where τ_{no} denotes the stress without control and τ_c with control. The effect of the amplitude of actuation (A) on D_r is examined and the results are shown in Fig. 2. The time scale of the actuation is fixed at $\Delta t_a^+ = 1.0$. As shown in Fig. 2, when A is smaller than $A = 0.125$, the effect of A on D_r is significant. D_r increases linearly with increasing A. However, as A increases further ($A > 0.125$), the effect of A on D_r is insignificant and D_r converges to $D_r \simeq 0.26$. This means that the higher amplitude of actuation ($A > 0.125$) is excessive and an optimum A exists at around $A \simeq 0.125$. Note that this optimum value of A in the present suboptimal control is close to the value of ϕ_{rms} in the active cancellation ($\phi_{rms} \simeq 0.121$).

The foregoing discussion indicates that the excessive amplitude of actuation ($A > 0.125$) gives the same drag reduction as that of the optimum actuation ($A = 0.125$). To see the effect of the excessive actuation, the near-wall flow structures are enlarged in Fig. 3. Two cases of actuation are chosen: one is the optimum ($A = 0.125$) and the other is the excessive actuation ($A = 0.30$). The case of no control ($A = 0$) is also displayed for comparison. In general, the turbulent intensities are weakened due to the control. The influence of the excessive actuation is distinctive in the distribution

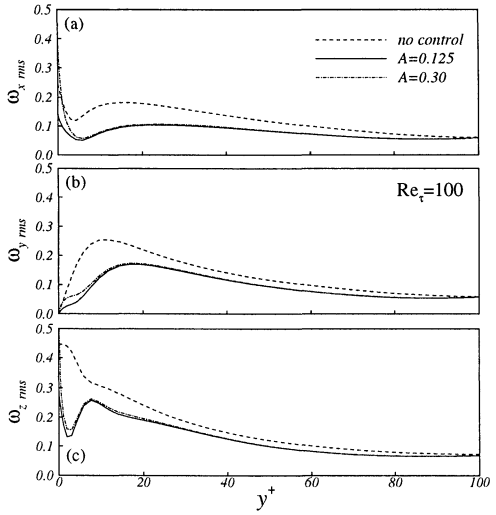

Fig. 4. Root-mean-squared vorticity distributions for ϕ_2 and $\partial w/\partial y|_w$. (a) $\omega_{x\ rms}$ (b) $\omega_{y\ rms}$ (c) $\omega_{z\ rms}$.

of normal turbulent intensity (v_{rms}) close to the wall ($y^+ \leq 20$) in Fig. 3(b). The increase of v_{rms} is expected by the direct wall normal actuation at the wall (ϕ_2). The spanwise turbulent intensity (w_{rms}) is seen to be slightly increased in Fig. 3(c), which is indirectly influenced by the mass conservation near the wall. Except for the near-wall region, the effect of the excessive actuation is insignificant and is confined to the region very close to the wall. Outside the near-wall region ($y^+ \geq 20$), the effect of the excessive actuation is almost negligible.

Comparison is extended to the distributions of root-mean-squared vorticity ($\omega_{i,\ rms}$). The global trend in Fig. 4 indicates that all three components of vorticity fluctuations are attenuated owing to the control. For $A = 0.30$, the wall vorticities ($\omega_{x,\ rms}$, $\omega_{z,\ rms}$) in the streamwise and spanwise directions are enhanced significantly very close to the wall. These values are even larger than that of no-control ($A = 0$). This is because the streamwise and spanwise wall actuation gradients ($\partial\phi_2/\partial x$, $\partial\phi_2/\partial z$) enhance the wall vorticities. The normal vorticity intensity ($\omega_{y,\ rms}$) near the wall is slightly enhanced due to the excessive actuation ($A = 0.30$). The increment of $\partial w/\partial x$ in the vicinity of the wall causes the enhancement of ω_y in the excessive control, i.e. , $\omega_y = \partial u/\partial z - \partial w/\partial x$. However, outside the near-wall region ($y^+ \geq 20$), two curves of $A = 0.125$ and $A = 0.30$ are almost the same. Since the streamwise vortices which play a key role in drag reduction are located outside the region ($y^+ \geq 20$), the drag reduction is not influenced by the excessive actuation ($A \geq 0.125$), although the power

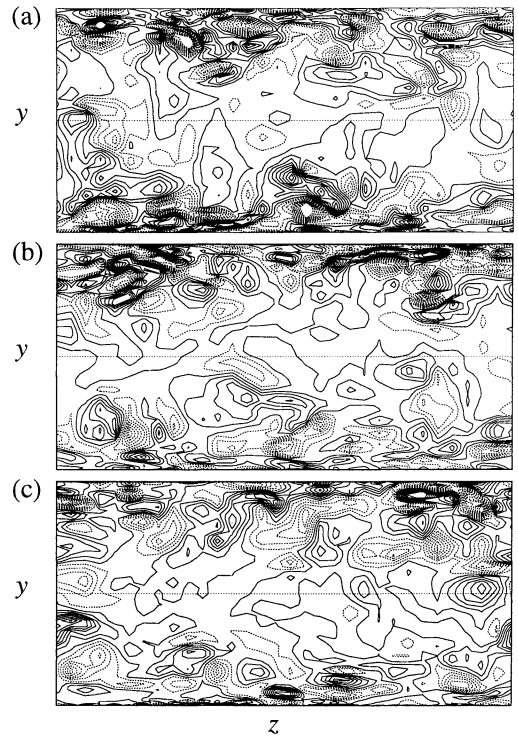

Fig. 5. Contours of ω_x in a cross-flow plane for ϕ_2 and $\partial w/\partial y|_w$. (a) $A = 0$ (b) $A = 0.125$ (c) $A = 0.30$.

of actuation is excessively imposed on the system.

To look into the effect of the excessive actuation in detail, instantaneous contours of ω_x in a cross-flow plane are illustrated in Fig. 5. For a no-control case ($A = 0$), many streamwise vorticities are crowded near the wall. When the optimal control ($A = 0.125$) is applied to the bottom wall, significant reduction in the strength of the streamwise vortices is evident. At the excessive control ($A = 0.30$), the general features are very similar to that of $A = 0.125$, except at the region in the vicinity of the wall. A closer inspection of the contours indicates that the streamwise vortices are densely crowded very close to the bottom wall by the excessive wall actuation.

Next, the wall actuation is changed to the wall sliding velocity (ϕ_3) in the control, $\partial w/\partial y|_w$ remains unchanged as a sensing variable. Similar to the prior test for ϕ_2, the active cancellations for three detection layers are tested at $y_d^+ = 5.9$, 9.6 and 14.2 to evaluate the amplitude of actuation (ϕ_3) in the suboptimal control. When the layer is detected at $y_d^+ = 9.6$, the asymptotic level of ϕ_{rms} converges to $\phi_{rms} \simeq 0.41$ in Fig. 6. If compared to the case of ϕ_2 in Fig. 1, the maximum drag reduction (τ_w) is obtained at $y_d^+ \simeq 9.6$. This means that the drag reduction rate depends

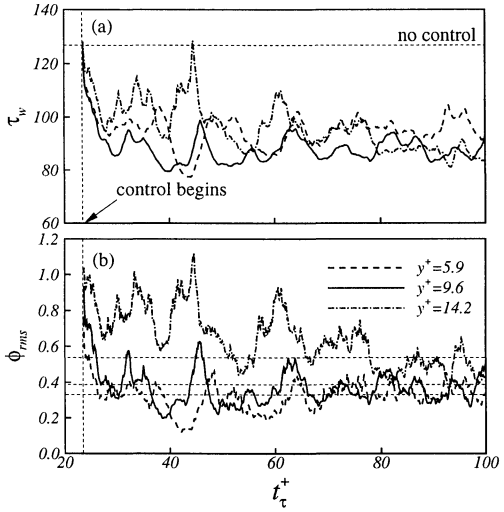

Fig. 6. Time history of (a) streamwise mean shear stress and (b) root-mean-squared values of actuation for ϕ_3.

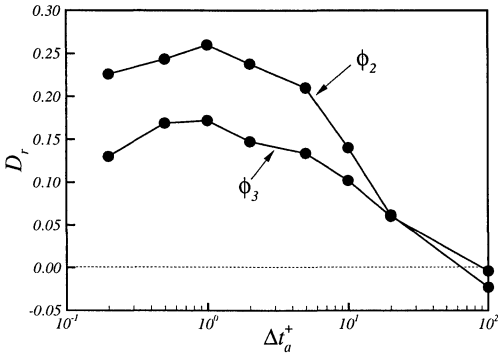

Fig. 7: Effect of Δt_a^+ on D_r for $\partial w/\partial y|_w$.

on the location of the detection layer, which is consistent with the result of Choi et al.(1994).

The influence of A on D_r for the ϕ_3 control is displayed in Fig. 2. The time scale of actuation is fixed at $\Delta t_a^+ = 1.0$. Within the range $A \leq 0.4$, the drag reduction rate (D_r) is linearly increased. However, when A is larger than 0.4, the drag reduction rate is stagnant. Thus, an optimum value is $A = 0.4$. It is interesting to see that this optimum value is close to the power of actuation (ϕ_{rms}) by the active cancellation at $y_d^+ = 9.6$.

As mentioned earlier, the phase information at a local time was obtained through a weight distribution between sensors and actuators in the control procedure of LKC. Since the control was confined to a spatial optimum in a control surface, the actuation time scale (Δt_a^+) was not considered. In the present study, the effect of the actuation time scale (Δt_a^+) is tested in Fig. 7. Two actuation cases (ϕ_2 and ϕ_3) are chosen. To see the influence of Δt_a^+ on D_r, the

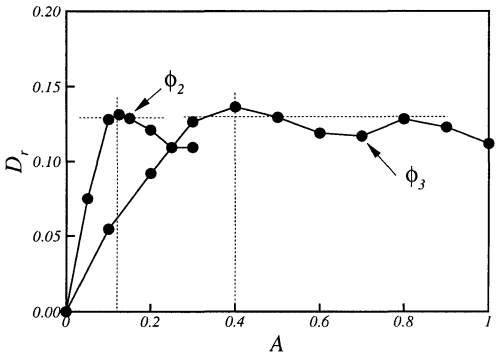

Fig. 8: Effect of A on D_r for $\partial p/\partial z|_w$.

amplitude of actuation (A) is fixed at the aforestated optimal value, i.e. , $A = 0.125$ for ϕ_2 and $A = 0.4$ for ϕ_3. As seen in Fig. 7, the drag reduction rate (D_r) is influenced by the actuation time scale significantly. An optimal time scale is obtained at $\Delta t_a^+ \simeq 1$ for both cases. This finding is important in terms of the realistic applications of the present suboptimal control. However, D_r decreases as Δt_a^+ increases further. In particular, when $\Delta t_a^+ \geq 100$, the drag is even increased. This suggests that the actuation time scale should be less than $\Delta t_a^+ \sim 100$. Note that this is consistent with the bursting period of Kim and Sparlart (1987).

In an effort to find another reliable wall sensing variable, the spanwise wall pressure gradient ($\partial p/\partial z|_w$) is considered as a footprint of ω_x above the wall. The wall suction and blowing for suppressing a streamwise vortex increases the pressure gradient in the spanwise direction under the streamwise vortex near the wall. It is known that the measurement of $\partial p/\partial z|_w$ is much easier in practice by using an array of pressure sensors (Lee and Sung, 1999). By utilizing $\partial p/\partial z|_w$ instead of $\partial w/\partial y|_w$, the same procedure is employed to see the influence of A and Δt_a^+ on D_r. The results for both ϕ_2 and ϕ_3 are displayed in Fig. 8. The time scale of actuation is fixed at $\Delta t_a^+ = 1.0$. Similar to the prior results of $\partial w/\partial y|_w$, optimal values of A are estimated at $A = 0.125$ for ϕ_2 and $A = 0.4$ for ϕ_3. Note that these optimal values are the same as the prior ones.

The effect of Δt_a^+ on D_r for both cases is exhibited in Fig. 9, where A is fixed at $A = 0.125$ for ϕ_2 and $A = 0.4$ for ϕ_3. It is seen that an optimal time scale is obtained at $\Delta t_a^+ = 1.0$ for both cases. As Δt_a^+ increases further, D_r decreases. When compared to the case of $\partial w/\partial y|_w$ in Fig. 7, D_r is very sensitive to the time scale in the region $\Delta t_a^+ < 1.0$ for ϕ_2 . A rapid change of D_r is observed in the re-

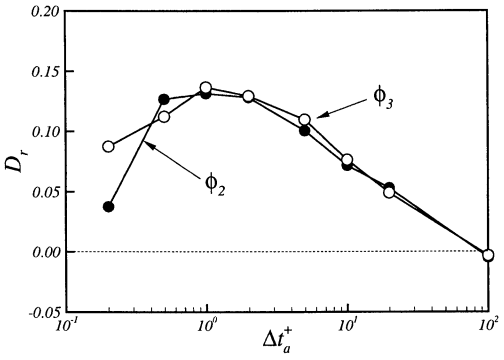

Fig. 9: Effect of Δt_a^+ on D_r for $\partial p/\partial z|_w$.

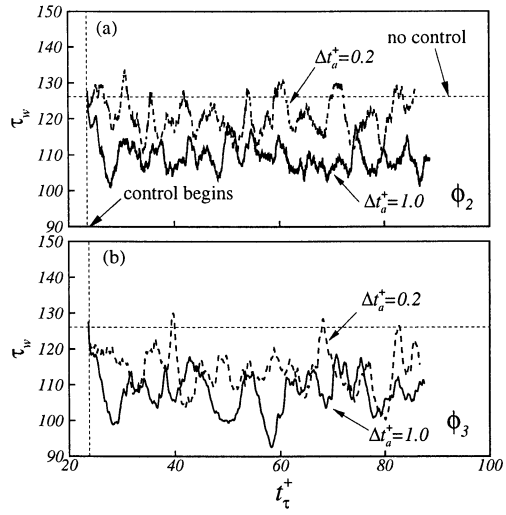

Fig. 10: Time history of τ_w for $\partial p/\partial z|_w$. (a) ϕ_2 (b) ϕ_3.

gion $0.2 < \Delta t_a^+ < 1.0$ in the case of ϕ_2. This means that the selection of Δt_a^+ in the region of $\Delta t_a^+ < 1.0$ should be careful in the realistic suboptimal control application by wall suction and blowing (ϕ_2). When $\Delta t_a^+ \geq 100$, the drag is even increased. This is similar to the case in Fig. 7.

The sensitivity of $\Delta t_a^+ = 0.2$ to τ_w is displayed in Fig. 10 by showing the time history of τ_w. Two control actuations (ϕ_2 and ϕ_3) are employed by sensing $\partial p/\partial z|_w$. The case of $\Delta t_a^+ = 1.0$ is included for comparison. It is evident that the response of τ_w to ϕ_2 is more sensitive than to ϕ_3. It is expected that the response of wall pressure fluctuations to the normal actuation ϕ_2 is more unstable in time than the case by the wall sliding velocity (ϕ_3). A closer inspection of the time history of τ_w in Fig. 10 indicates that small fluctuations of τ_w for the trajectories of ϕ_2 are included while the trajectories of ϕ_3 are not. This may be attributed to the fact that some corrupted phases are contaminated between the wall normal actuation and the wall pressure ($\partial p/\partial z|_w$).

CONCLUSION

Detailed numerical analyses have been performed to delineate the suboptimal control laws for drag reduction. The influence of the amplitude of actuation (A) and the time scale of actuation (Δt_a^+) was evaluated for two sensing parameters, $\partial w/\partial y|_w$ and $\partial p/\partial z|_w$, with two actuations ϕ_2 and ϕ_3. Active cancellation was employed to validate the effective amplitude of actuation. It was found that an optimum A exists for a given control set. The excessive amplitude of actuation gives the same drag reduction as that of optimum actuation. The effective actuation is confined to the region very close to the wall ($y^+ \leq 20$). The drag reduction rate by ϕ_3 is slightly lower than that by ϕ_2. An optimal time scale is obtained at $\Delta t_a^+ \simeq 1$ and Δt_a^+ should be less than $\Delta t_a^+ \sim 100$. The most effective drag reduction is achieved at the pair of ϕ_2 and $\partial w/\partial y|_w$.

REFERENCES

Bewley, T.R., Choi, H., Temam, R. and Moin, P., 1993, "Optimal Feedback Control of Turbulent Flow", CTR, Annual Research Brief, pp.3-13.

Choi, H., Moin P. and Kim, J., 1994, "Active Turbulence Control for Drag Reduction in Wall-Bounded Flows", *J. Fluid Mech.*, Vol. 262, pp.75-110.

Hammond, E.P., Bewley, T.R. and Moin, P., 1998, "Observed Mechanisms for Turbulence Attenuation and Enhancement in Opposition-Controlled Wall-Bounded Flows", *Phys. Fluids*, Vol. 10, pp.2421-2423.

Kim, J. and Sparlart, P.R., 1987, "Scaling of the Bursting Frequency in Turbulent Boundary Layers at Low Reynolds Numbers", *Phys. Fluids*, Vol. 30, pp.3326-3328.

Kim, J., Moin, P. and Moser, R.K., 1987, "Turbulence Statistics in Fully Developed Channel Flow at Low Reynolds Number", *J. Fluid Mech.*, Vol. 177, pp.133-166.

Kim. J, 1989, "On the Structure of Pressure Fluctuations in Simulated Turbulent Channel Flow", *J. Fluid Mech.* Vol. 205, pp.421-451.

Lee, C., Kim, J. and Choi, H., 1998, "Suboptimal Control of Turbulent Channel Flow for Drag Reduction", *J. Fluid Mech.*, Vol. 358, pp.245-258.

Lee, I. and Sung, H.J., 1999, "Development of an Array of Pressure Sensors with PVDF Film", *Exp. Fluids*, Vol. 26, pp.27-35.